**ORIGINAL ARTICLE**

# Stretchable π-conjugated polymer electrets for mechanoelectric generators

Akira Shinohara[1] · Manabu Yoshida[2] · Chengjun Pan[3] · Takashi Nakanishi [1]

## Abstract

Electrets are materials that retain quasi-permanent electric charges and are attracting attention as key components of batteryless micropower supplies. A chemical structure that facilitates ionization and that can stabilize these charges, such as a π-conjugated system, is expected to increase the charge density compared with that of conventional insulating polymers. Here, we report a mechanoelectric generator (MEG) (vibrational energy harvester) that uses alkylated π-conjugated polymers (Alk-CPs), which can be monopolarized either into positive or negative mode electrets. With the attachment of insulating, bulky, yet flexible alkyl side chains to the π-conjugated backbone, the poled Alk-CPs showed long charge lifetime suitable for MEGs. The elastic modulus of the electret was adjusted to approximately match that of the stretchable polyurethane substrate by blending two miscible Alk-CPs with different elastic moduli, producing a laminated film that could be stretched up to 300%. The MEG presented showed conformability when applied to a deformable object.

## Introduction

Electrets are monopolarized or bipolarized dielectrics that have been quasi-permanently charged by various methods. Applications of these electrical counterparts of magnets are rather limited, even though more than one hundred years have passed since they were first experimentally demonstrated [1]. For example, the idea of power generation with electrets has been around for a long time, but the corresponding output is small (Supplementary Note 1).

✉ Takashi Nakanishi
NAKANISHI.Takashi@nims.go.jp

1 International Center for Materials Nanoarchitectonics (WPI-MANA), National Institute for Materials Science (NIMS), 1-1 Namiki, Tsukuba 305-0044, Japan

2 Sensing System Research Center, National Institute of Advanced Industrial Science and Technology (AIST), 1-1-1 Umezono, Tsukuba 305-8565, Japan

3 Shenzhen Key Laboratory of Polymer Science and Technology, College of Materials Science and Engineering, Shenzhen University, 1066 Xueyuan Boulevard, Nanshan, Shenzhen 518055, China

Nevertheless, electret-based mechanoelectric generators (MEGs), which convert mechanical force to electricity *via* electrostatic induction, have continued to attract the interest of researchers because they exhibit some unique properties that are not seen in chemical batteries. First, the ideal MEG has an infinite lifetime based on its mechanism of operation, although in reality, the lifetime of the device is determined by the lifetime of the charge in the electret. Second, MEGs do not require an electrolyte and possess high impedance and thus are thought to be safe for human-adaptive power supplies. In recent years, with improvements in the performance of MEGs [2, 3] along with the miniaturization and power savings of electronic devices, various practical applications for MEGs, such as wearable devices [4–6], sensors [7, 8], and transmitters [9], have emerged.

How long the charge of electrets can be retained is an area of concern. To prevent the loss of trapped charges due to self-discharge, highly insulating polymers such as fluoropolymers [10], polyamides [11], and polyolefins [12] are often used. Of the various methods used for mono/bipolarization, which is called poling [13], ambient-atmosphere corona discharge is a simple method that enables poling in a short time. Molecules in the atmosphere are ionized by high voltage, and the resulting ions collide with the polymers to generate a monopole (and in some cases, a dipole induced by it). (Supplementary Note 2).

Although the actual species of trapped charges in the electrets are not well understood, they are believed to consist of the impacting ions themselves or oxidation/reduction products formed by subsequent reaction with the polymers.

Another concern is how to increase the density of the charges trapped in an electret. Compared to the electronically inactive polymers described above, $\pi$-conjugated molecules and polymers are expected to trap charges with greater thermodynamic stability because they easily ionize [14]. By taking advantage of this feature, several $\pi$-electrets, including perylene diimides [15], phthalocyanines [16, 17], and $\pi$-conjugated polymers [18–20], have been designed for organic field effect transistor (OFET) memories. However, $\pi$-electrets exhibit relatively high electrical conductivity, resulting in a short lifetime for trapped charges due to self-discharge, and thus are considered unsuitable for MEGs [21]. This lifetime can be improved by insulation or isolation of the $\pi$-conjugated unit at the molecular level by alkyl side chains or polymeric matrices, which is also advantageous for application to flexible devices [22, 23]. Recently, we proposed stretchable MEGs using porphyrins as $\pi$-electrets, where the porphyrins are liquefied at room temperature by peripherally attached bulky yet flexible alkyl chains [24]. The present work describes the first $\pi$-conjugated polymer-based MEGs, whose trapped charges are stabilized by insulating alkyl side chains. We highlight a unique feature of these alkylated $\pi$-conjugated polymers (Alk-CPs), that the modulus of the $\pi$-electrets can be adjusted by blending two miscible Alk-CPs [25], thus providing the assembled MEGs with excellent stretchability.

## Experimental procedure

### Materials

Alk-CPs **P1** and **P2** were synthesized as previously reported [25]. The molecular weight and its distribution were determined by gel permeation chromatography using a Shimadzu Nexera GPC system equipped with a column (Shim-pack GPC-80M, 300 mm length × 8 mm diameter, exclusion limit $2 \times 10^7$ Da). The number-average molecular weights ($M_n$), weight-average molecular weight ($M_w$), and polydispersity index (PDI $= M_w/M_n$) referenced to polystyrene standards (TSKgel, Tosoh Corporation, Japan) were as follows. **P1**: $M_n = 10.4$ kDa, $M_w = 18.6$ kDa, PDI $= 1.78$; **P2**: $M_n = 10.6$ kDa, $M_w = 19.6$ kDa, PDI $= 1.84$. The Alk-CP blend **B1** was prepared by dissolving equimass **P1** and **P2** in a small amount of chloroform and then drying under vacuum at 150 °C overnight.

## Alk-CP film preparation

Weighed Alk-CP (10 mg) was heated under vacuum to remove bubbles, placed between two polyimide (PI) films (Kapton®, 12.5 μm thickness) with aluminum foil spacers (4 × 12 μm) and slowly pressed at 100 °C (**P1**), 60 °C (**B1**), or room temperature (20 °C, **P2**) with a pressure of 10 MPa using a hot press machine (MP-SCH, Toyo Seiki Seisakusho, Ltd., Japan). One PI film was peeled off under proper cooling, and another PI film was cut to the same size as the Alk-CP film. The laminated films were used for screening experiments on the poling conditions (i.e., surface potential measurements). For MEG fabrication, the Alk-CP film on the PI film was transferred onto porous polytetrafluoroethylene (pPTFE) film (Poreflon®, Sumitomo Electric Industries Ltd., Japan, 0.5 μm pore size, 30 μm thickness) by pressing at the same temperature as the press molding with a lower pressure of 1 MPa.

## Surface potential measurement

The Alk-CP/PI film was placed on a fluorinated tin oxide (FTO) glass substrate (25 × 25 mm) and poled at various temperatures (20, 60, and 100 °C) and durations (1, 5, and 15 min). The poling was performed using a corona discharging gun (GC90PN, Green Techno Co., Ltd., Japan) placed perpendicular to a grounded stainless steel plate (200 × 200 mm). The poling temperature was controlled by a hot plate (ND-2A, AS ONE Corp., Japan). The electrode–sample distance was fixed at 200 mm, and the applied voltage was ±80 kV. The surface potential was measured at room temperature (at approximately 20 °C with a relative humidity of 60–70%) using an electrostatic analyzer (Keyence SK-100) with a sample–probe distance of 15 mm (air scaling factor $= 1.00$, detection area $= \varphi 60$ mm). The obtained surface potential values were corrected in terms of the detection area with a proportional factor of 2.24, which was determined by measuring the surface potential of the poled PI films with different diameters.

## Fabrication of MEG

A stretchable electrode was fabricated on polyurethane (Breath Roll® BR15, Nitto Co., Ltd., Japan, 13 μm thickness) by applying silver-plated nylon fibers (AGposs®, Mitsufuji Co., Ltd., Japan, fiber length = 3 mm). The typical resistance of the electrode was <5 Ω. The poling of the Alk-CP/pPTFE laminated film was performed on the electrode at 60 °C for 15 min using the procedure described above. After placing a polyurethane (PU) spacer, the active area of the electret was sealed by another electrode. Successful assembly of the MEG was confirmed by insulation between two electrodes with a resistance of >40 MΩ. The

**Fig. 1 a** Chemical structures of Alk-CPs **P1** and **P2**. **b** Stretching of Alk-CP films laminated on polyurethane (PU) elastomer film
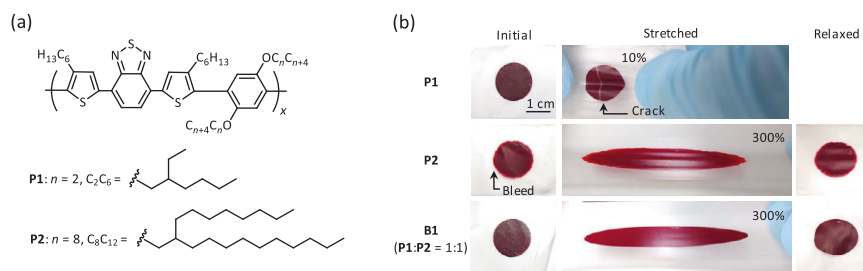


open circuit voltage ($V_{oc}$) of working MEGs was recorded on an oscilloscope (MT-775, MotherTool Co., Ltd., Japan) equipped with a probe with an input impedance of 1 MΩ. The top electrode of the MEG was connected to the probe, and the bottom electrode was grounded.

## Results and discussion

### Preparation of π-electrets

Donor–acceptor alternating copolymers, composed of electron-deficient benzothiadiazole units and electron-rich dialkoxybenzene units [25], were used as π-electrets (Fig. 1a). Branched alkyl chains with a branch at the 2-position, the so-called Guerbet chains ($C_nC_{n+4}$), are highly capable of softening and amorphizing rigid π-conjugated molecules [26–30] and polymers [25, 31, 32] and enable a wide range of elastic modulus ($G'$) tunability. **P1**, with short side chains ($n = 2$), is a glass at room temperature ($T_g = 29\,°C$), while **P2**, with long side chains ($n = 8$), is a liquid ($T_g = -29\,°C$). Both Alk-CPs are highly insulating for two reasons. One reason is their amorphousness; the absence of long-range ordering makes interchain conduction such as carrier hopping less likely to occur. The other is insulation by the alkyl side chains, which also suppress interchain conduction.

Figure 1b shows stretching tests of the Alk-CPs laminated with PU elastomer substrate. A uniform thin film of the Alk-CPs (with thickness of approximately 50 µm) can be easily obtained by using a hot press machine (*vide* Experimental Procedure). The glassy **P1** ($G'$ approximately $10^8$ Pa) that transfers to the PU film easily cracks under tensile deformation even with a small elongation (10%), whereas the liquid **P2** ($G'$ approximately $10^4$ Pa) can be stretched without any cracking until the substrate breaks (>300%). However, since the liquid has no shape retention, it will bleed onto the substrate within 24 h after lamination. **P1** and **P2** are miscible with each other [25], and the elastic modulus can be adjusted by the blend ratio

to obtain an elastic modulus close to that of the substrate. The equimass blend (**B1**) is rubbery at room temperature ($G'$ approximately $10^6$ Pa), similar to the PU substrate, and achieves both shape retention and deformation conformability (300%) in the laminated film (Supplementary Movie 1).

### Charge retention

Prior to MEG fabrication, we investigated the charge retention of the π-electret films (**P1**, **P2**, and **B1**) poled with ambient-atmosphere corona discharge at different temperatures (20, 60, and 100 °C) (Fig. 2). The surface potential ($V_s$) was saturated after a short time of poling (<approximately 15 min) (Fig. S1), which was of the same polarity (homocharge) as the applied voltage, suggesting that the retained charge evolved from the injected active species. In general, electrets have different positive and negative charge retention characteristics depending on their electron energy band structure, such as band gap and trap depth [33]. Since the present Alk-CPs have a donor–acceptor architecture, π-electrets of either positive or negative polarity could be produced. Except for the case of poling temperature $T = 20\,°C$, the surface potentials of the different samples were ordered **P2** > **B1** > **P1**. As representative results, when $T = 60\,°C$ in positive mode (Fig. 2b), the initial $V_s$ and potential retention after 30 min were 0.75 kV/68% (**P1**), 0.93 kV/77% (**P2**), and 0.85 kV/76% (**B1**), respectively. This trend is likely related to the mass composition ratio of alkyl chains, which can prevent the loss of surface charge due to self-discharge by insulation [21].

It is also believed that the reduction in the elastic modulus upon heating aids charge diffusion into the electret and promotes thermally driven charge injection processes, allowing a higher volumetric charge density and stable charge retention to be achieved. For this reason, electret poling is routinely performed under heat [34]. Charge injection efficiency was found to be dependent on elastic modulus in our previous work [24]; under the same conditions, materials with lower elastic moduli were more
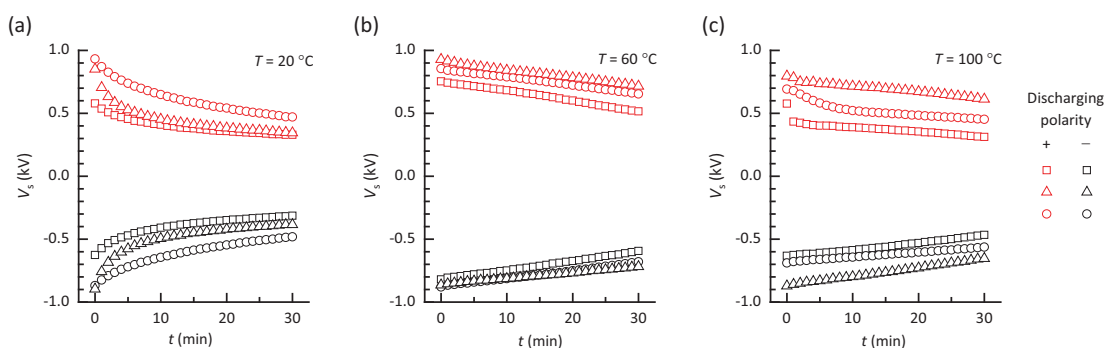
**Fig. 2** Surface potential ($V_s$) decay (at 20 °C) of π-electret films (**P1**, **P2**, and **B1**) poled at different temperatures. **a** 20 °C, **b** 60 °C, and **c** 100 °C. Poling time: 15 min ($T = 20$ and 60 °C); 5 min (100 °C)



**Fig. 3 a** Structure (left) and photograph (right) of a single mechanoelectric generator cell. **b** Deformability in stretching (left), twisting (middle), and folding (right) (inset shows origami crane folded from a single device) modes
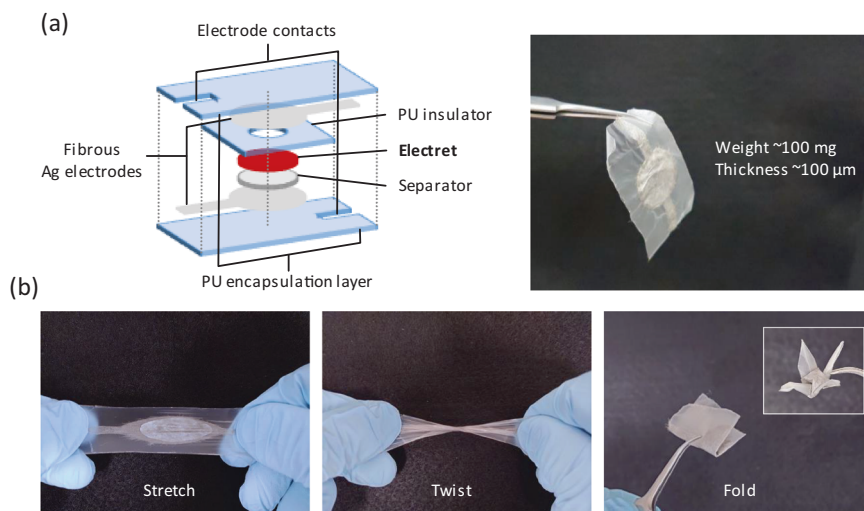
likely to be poled. However, the charge retention of the present Alk-CPs was the highest at 60 °C, suggesting that the charge injection efficiency is nearly independent of the elastic modulus and unique to the π-conjugated backbone chemical structure. A slight decrease in charge retention at 100 °C was observed. This may be due to the thermal enhancement of electrical conduction [35]. (Supplementary Note 3) causing charge loss, which competes with the charge injection process; this needs to be clarified in the future together with the poling mechanism.

## Fabrication of MEGs

Figure 3a shows the structure of a fabricated MEG. A π-electret layer, a porous polytetrafluoroethylene (pPTFE) separator, and a PU insulator/spacer are laminated between two stretchable silver electrodes. The assembled MEG weighs only approximately 100 mg and has a thickness of approximately 100 μm for an active area of 78.5 mm$^2$ (=10 mm diameter of hole in PU insulator). A review of the

constituent materials may make it possible to further increase the active area and reduce the weight and thickness. Except for the case where the glassy **P1** is used, the entire assembled MEG is flexible and can be deformed in stretching, twisting, and folding modes (Fig. 3b and Supplementary Movie 2).

To evaluate the output characteristics of the fabricated MEGs, we investigate the change in potential difference between the top and bottom electrodes when a wooden ball (diameter = 16 mm; weight $m = 1.57$ g; $mgh = mv = 0.154$ mJ for initial height $h = 100$ mm, $g$ and $v$ are the gravitational acceleration and impact rate, respectively) is dropped onto the MEGs (Fig. 4a). The single induction shows a bipolar open circuit voltage ($V_{oc}$), which is phase-reversed by the poling polarity of the electret (Fig. 4b). This is consistent with a possible operating principle, the so-called contact–separation mode [2]. That is, in an MEG with a positive electret, the induced (compensating) charge moves from the bottom electrode to the top electrode due to the change in the distance between the top electrode and the
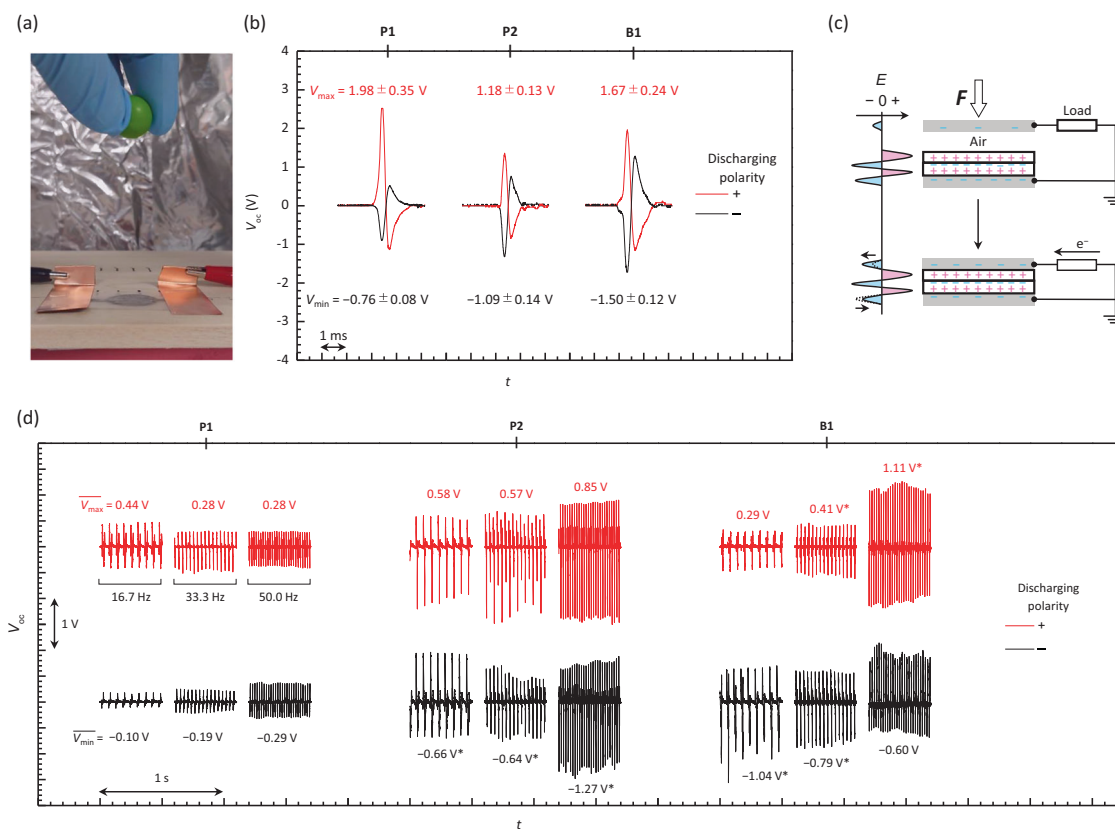
**Fig. 4 a** Photograph of a single induction experiment consisting of dropping a wooden ball onto the fabricated mechanoelectric generator (MEG). **b** Open circuit voltages ($V_{oc}$) generated by the MEGs. MEGs were placed on a wooden plate, and a wooden sphere was dropped onto the top electrode from a height ($h$) of 100 mm (weight of the wooden sphere $m = 1.57$ g, $mgh = 0.154$ mJ). The average maximum voltage ($V_{max}$, for positive mode MEG) and minimum voltage ($V_{min}$, for negative mode MEG) were taken from five tests, and errors were represented by a standard deviation (1 SD). **c** Possible operation mechanism of the MEG in contact–separation mode and electric field strength ($E$) distribution along the thickness direction. **d** $V_{oc}$ of MEGs under continuous vibration with different frequencies. An asterisk (*) on the value indicates that the polarity of the output is reversed from that of the single induction experiment

electret layer (i.e., the current is directed from the top electrode to the bottom electrode) (Fig. 4c). During relaxation, an opposite direction current flows, and the time integral of the voltage equals zero. No significant difference is observed among the amplitudes of the $V_{oc}$ of the Alk-CPs (positive mode: $V_{max} = 1.98$ V (**P1**); 1.18 V (**P2**); 1.67 V (**B1**), negative mode: $V_{min} = -0.76$ V (**P1**); $-1.09$ V (**P2**); $-1.50$ V (**B1**)), indicating that elastic modulus tailoring is possible while maintaining charge retaining properties. The induction performance remains at 7–42% of the initial value after 37 days, confirming the charge retention of the present π-electrets (Table S1). Long-term retention characteristics will be investigated further in a future study.

Under continuous vibration (frequency = 16.7, 33.3, and 50 Hz), no significant differences in the average amplitude of $V_{oc}$ are observed depending on the electret poling polarity and vibration frequency (positive mode: $V_{max} = 0.24$ to 0.28 V (**P1**); 0.57 to 0.85 V (**P2**); 0.29 to 1.11 V (**B1**), negative mode: $V_{min} = -0.10$ to $-0.29$ V (**P1**); $-0.64$ to $-1.27$ V (**P2**); $-0.60$ to $-1.04$ V (**B1**))

(Fig. 4d). Unlike the above single induction experiment, **P2** and **B1** show larger amplitudes than **P1**; however, the reason for this observation is not clear. In some of the tests we conduct, the $V_{oc}$ polarities are inverted, suggesting that they originate from something other than the charge injected by corona discharge. For example, applied pressure can induce triboelectric series-determined charges at the separator–electret interface. Notably, the MEG retains its original polarities after the continuous vibration test, suggesting that this phenomenon originates from transient induced charges.

## Object-conformable mechanoelectric generation

According to the principle of mechanoelectric generation, the waveform of the output $V_{oc}$ depends on the deformation velocity of the MEG; in the contact–separation mode, it corresponds to the rate of change of the top electrode–electret distance. Since the MEG presented is stretchable, it can adapt to the deformation of the object on

**Fig. 5 a** Single induction experiment consisting of dropping a wooden ball using different floor materials: wood (left) and PU foam (right). **b** The output open circuit voltage ($V_{oc}$) related to the indentation depth $x$. When the MEG is applied on soft floor material (i.e., PU foam), the signal is broadened corresponding to the deceleration rates ($\dot{v}$) of the ball
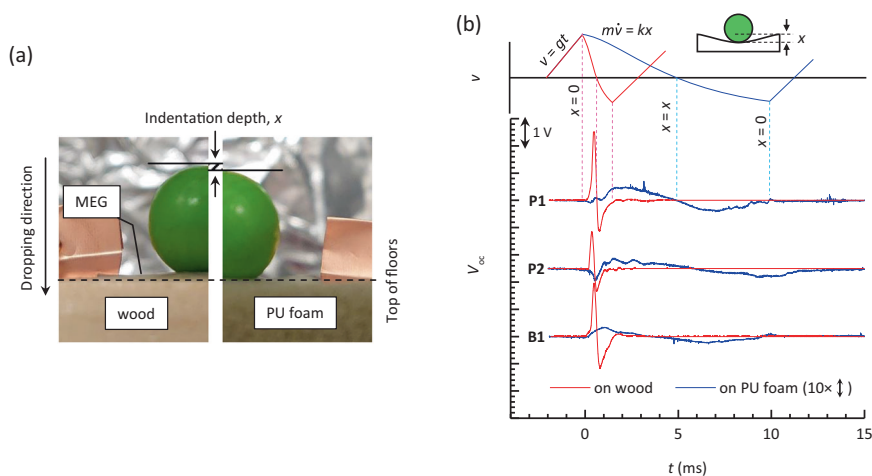


which it is placed. We, therefore, conduct a ball drop experiment using floor materials with different hardnesses (Fig. 5a). With a relatively hard floor (wood), the peak width is less than 1 ms, while with a relatively soft floor (PU foam), the signal broadens to approximately 5 ms (Fig. 5b). This difference in signal width corresponds to the deceleration rate ($\dot{v}$) of the ball. That is, the ball decelerates only within the thickness of the MEG upon impact on the hard floor (ignoring the ball and floor deformation), but on the soft floor, it takes longer to decelerate due to indentation. Such dynamic properties are not found in MEGs fabricated on typical inelastic substrates such as FTO electrodes.

## Conclusions

In summary, mechanoelectric generators (MEGs) using alkylated π-conjugated polymer (Alk-CP) electrets were successfully produced and demonstrated. The charge retention properties of the π-electrets slightly decreased with the elastic modulus (i.e., **P2 > B1 > P1**), which was adjusted by blending glassy and liquid miscible Alk-CPs. This simple method of matching the elastic modulus with that of other laminated materials endowed the MEGs with excellent stretching of up to 300% and deformability in different modes such as twisting and folding. The object conformability of the MEGs, which was a result of their deformability, enabled the detection of not only displacement but also time-dimensional information, which is difficult to achieve with conventional hard and inelastic devices. Thus, the MEGs are expected to be useful in future sensing applications such as soft robotics and haptics.

## Compliance with ethical standards

**Conflict of interest** The authors declare no competing interests.

## References

1. Eguchi M. Variation of electrical conductivity of oils and waxes. Proc Phys-Math Soc Jpn Ser. 1919;1:320–6.
2. Liu R, Wang ZL, Fukuda K, Someya T. Flexible self-charging power sources. Nat Rev Mater. 2022. https://doi.org/10.1038/s41578-022-00441-0.
3. Persano L, Ghosh SK, Pisignano D. Enhancement and function of the piezoelectric effect in polymer nanofibers. Acc Mater Res. 2022;3:900–12.
4. Ryu H, Park HM, Kim MK, Kim B, Myoung HS, Kim TY, et al. Self-rechargeable cardiac pacemaker system with triboelectric nanogenerators. Nat Commun. 2021;12:4374.
5. Jiang D, Shi B, Ouyang H, Fan Y, Wang ZL, Li Z, et al. Emerging implantable energy harvesters and self-powered implantable medical electronics. ACS Nano. 2020;14:6436–48.
6. Wan X, Chen P, Xu Z, Mo X, Jin H, Yang W, et al. Hybrid-piezoelectret based highly efficient ultrasonic energy harvester for implantable electronics. Adv Funct Mater. 2022;32:2200589.

7. Park S, Kim H, Vosgueritchian M, Cheon S, Kim H, Koo JH, et al. Stretchable energy-harvesting tactile electronic skin capable of differentiating multiple mechanical stimuli modes. Adv Mater. 2014;26:7324–32.

8. Chortos A, Liu J, Bao Z. Pursuing prosthetic electronic skin. Nat Mater. 2016;15:937–50.

9. Cui Y, Wu M, Li Z, Song X, Wang C, Yuan H, et al. A miniaturized mechanical antenna based on FEP/THV unipolar electrets for extremely low frequency transmission. Microsyst Nanoeng. 2022;8:58.

10. Schröder S, Strunskus T, Rehders S, Gleason KK, Faupel F. Tunable polytetrafluoroethylene electret films with extraordinary charge stability synthesized by initiated chemical vapor deposition for organic electronics applications. Sci Rep. 2019;9:2237.

11. Zhu J, Ma F, Zhu H. Single-electrode, nylon-fiber-enhanced polytetrafluoroethylene electret film with hollow cylinder structure for mechanical energy harvesting. Energy Technol. 2018;6:1112–8.

12. Xu J, Xu L, Zheng N, Yang J, Jiang Z, Zhang C, et al. Controllable preparation of porous polypropylene piezoelectrets using crystallization self-reinforcement method induced by the variable thermal history. Macromol Mater Eng. 2022;307:2200314.

13. Guo Z, Patil Y, Shinohara A, Nagura K, Yoshida M, Nakanishi T. Organic molecular and polymeric electrets toward soft electronics. Mol Syst Des Eng. 2022;7:537–52.

14. Duhm S, Heimel G, Salzmann I, Glowatzki H, Johnson RL, Vollmer A, et al. Orientation-dependent ionization energies and interface dipoles in ordered molecular assemblies. Nat Mater. 2008;7:326–32.

15. Ho CH, Lin TC, Yang WC, Ercan E, Chiang YC, Lin BH, et al. Fast photoresponsive phototransistor memory using star-shaped conjugated rod–coil molecules as a floating gate. ACS Appl Mater Interfaces. 2022;14:15468–77.

16. Aimi J, Lo CT, Wu HC, Huang CF, Nakanishi T, Takeuchi M, et al. Phthalocyanine-cored star-shaped polystyrene for nano floating gate in nonvolatile organic transistor memory device. Adv Electron Mater. 2016;2:1500300.

17. Aimi J, Yasuda T, Huang CF, Yoshio M, Chen WC. Fabrication of solution-processable OFET memory using a nano-floating gate based on a phthalocyanine-cored star-shaped polymer. Mater Adv. 2022;3:3128–34.

18. Chen C, Wang Y, Tatsumi H, Michinobu T, Chang SW, Chiu YC, et al. Novel photoinduced recovery of OFET memories based on ambipolar polymer electret for photorecorder application. Adv Funct Mater. 2019;29:1902991.

19. Chang TW, Li YS, Matsuhisa N, Shih CC. Emerging polymer electrets for transistor-structured memory devices and artificial synapses. J Mater Chem C 2022;10:13372–94.

20. Chen CH, Wang Y, Michinobu T, Chang SW, Chiu YC, Ke CY, et al. Donor–acceptor effect of carbazole-based conjugated polymer electrets on photoresponsive flash organic field-effect transistor memories. ACS Appl Mater Interfaces. 2020; 12:6144–50.

21. Moretti G, Rosset S, Vertechy R, Anderson I, Fontana M. A review of dielectric elastomer generator systems. Adv Intell Syst. 2020;2:2000125.

22. Zheng Y, Zhang S, Tok JBH, Bao Z. Molecular design of stretchable polymer semiconductors: current progress and future directions. J Am Chem Soc. 2022;144:4699–715.

23. Higashihara T. Strategic design and synthesis of π-conjugated polymers suitable as intrinsically stretchable semiconducting materials. Polym J. 2021;53:1061–71.

24. Ghosh A, Yoshida M, Suemori K, Isago H, Kobayashi N, Mizutani Y, et al. Soft chromophore featured liquid porphyrins and their utilization toward liquid electret applications. Nat Commun. 2019;10:4210.

25. Guo Z, Shinohara A, Pan C, Stadler FJ, Liu Z, Yan ZC, et al. Consistent red luminescence in π-conjugated polymers with tuneable elastic moduli over five orders of magnitude. Mater Horiz. 2020;7:1421–26.

26. Babu SS, Aimi J, Ozawa H, Shirahata N, Saeki A, Seki S, et al. Solvent-free luminescent organic liquids. Angew Chem Int Ed. 2012;51:3391–95.

27. Babu SS, Hollamby MJ, Aimi J, Ozawa H, Saeki A, Seki S, et al. Nonvolatile liquid anthracenes for facile full-colour luminescence tuning at single blue-light excitation. Nat Commun. 2013;4:1969.

28. Lu F, Takaya T, Iwata K, Kawamura I, Saeki A, Ishii M, et al. A Guide to design functional molecular liquids with tailorable properties using pyrene-fluorescence as a probe. Sci Rep. 2017;7:3416.

29. Neal EA, Nakanishi T. Alkyl-fullerene materials of tunable morphology and function. Bull Chem Soc Jpn. 2021;94:1769–88.

30. Machida T, Nakanishi T. Alkyl-π functional molecular liquids towards soft electronics. J Mater Chem C. 2021;9:10661–7.

31. Shinohara A, Guo Z, Pan C, Nakanishi T. Solvent-free conjugated polymer fluids with optical functions. Org Mater. 2021;3:309–20.

32. Shinohara A, Pan C, Guo Z, Zhou L, Liu Z, Du L, et al. Viscoelastic conjugated polymer fluids. Angew Chem Int Ed. 2019;58:9581–5.

33. Takada T, Kikuchi H, Miyake H, Tanaka Y, Yoshida M, Hayase Y, et al. Determination of charge-trapping sites in saturated and aromatic polymers by quantum chemical calculation. IEEE Trans Dielectr Electr Insul. 2015;22:1240–9.

34. Sohrabi M, Komijani A. Surface potential stability of large-area Teflon PTFE electret dosimeters of different thicknesses. J Instrum. 2018;13:P06013.

35. Chen XB, Issi JP, Cassart M, Devaux J, Billaud D. Temperature dependence of the conductivity in conducting polymer composites. Polymer. 1994;35:5256–8.